

# Photoinduced dissociation reactions of silver fluoride cluster ions

N. Hori, A. Furuya, M. Tsuruta, F. Misaizu<sup>a</sup>, and K. Ohno

Department of Chemistry, Graduate School of Science, Tohoku University, Aramaki, Aoba-ku, Sendai 980-8578, Japan

Received 23 July 2006 / Received in final form 18 October 2006

Published online 24 May 2007 – © EDP Sciences, Società Italiana di Fisica, Springer-Verlag 2007

**Abstract.** Photoinduced dissociation in the ultraviolet region has been investigated for  $\text{Ag}_n\text{F}_{n-1}^+$  cluster ions. Photodissociation spectrum of  $\text{Ag}_2\text{F}^+$  in the energy of 3.8–5.6 eV exhibits several sharp bands corresponding to the transition to electronically excited states. In this dissociation, only the  $\text{Ag}_2^+$  ion was observed as a fragment ion. Theoretical calculation indicates that the parent  $\text{Ag}_2\text{F}^+$  ion has a linear Ag-F-Ag equilibrium geometries in the ground and excited states. Since conformational changes by excitation of bending vibration are necessary for the fragmentation of an F atom, this indicates that production of  $\text{Ag}_2^+$  from  $\text{Ag}_2\text{F}^+$  is a result of internal conversion and following conformational changes.

**PACS.** 36.40.Mr Spectroscopy and geometrical structure of clusters – 36.40.Qv Stability and fragmentation of clusters

## 1 Introduction

Halogenated coinage metals have attracted much interest for many decades because of their many practical applications. They exhibit various interesting properties depending on their metal-halogen compositions, such as powerful oxidizing properties of  $\text{AgF}_3$  [1] and generation of ultraviolet entangled photon pairs in a single crystal of the semiconductor  $\text{CuCl}$  [2]. Among them, silver halide compounds are well-known as photosensitive materials in photographic industry. In order to understand processes on photographic films, plates or papers, photochemistry of silver bromide and chloride has been studied for many years [3,4]. Recently, in order to get information on such unique properties of the compounds with microscopic level, the photophysics of silver halide clusters, especially of silver bromide clusters [5,6], was examined by gas-phase spectroscopic techniques. The metastable fragmentation channels of silver bromide cluster cations were reported by L'Hermite et al. [7,8], and several studies about the spectroscopic properties of silver monohalide clusters were reported [9,10]. Recently, theoretical studies were also performed to investigate the geometrical structures and stabilities of silver halide clusters [11–14].

In this study, we have applied mass-selected photodissociation of silver fluoride cluster ions,  $\text{Ag}_n\text{F}_{n-1}^+$ , in order to investigate their excited electronic states and photoinduced dissociation processes. In photodissociation of  $\text{Ag}_n\text{F}_{n-1}^+$  ( $n = 2-8$ ) at 266 nm, there is a clear difference of main fragmentation pathways between  $n = 2$  and larger sizes. The excited electronic states and the geometrical structure of  $\text{Ag}_2\text{F}^+$  are also discussed from the ob-

tained photodissociation spectrum in comparison with the theoretical calculation based on density-functional-theory (DFT). We will also discuss the photodissociation mechanism of  $\text{Ag}_2\text{F}^+$ .

## 2 Experiment

The experimental setup consists of three-stage differentially evacuated chambers, containing a cluster source, acceleration electrodes of a time-of-flight (TOF) mass spectrometer and a reflectron TOF mass spectrometer, respectively. Silver fluoride cluster ions were formed by combination of laser vaporization and supersonic expansion in the first chamber. The second harmonic of a Nd:YAG (New Wave, Tempest-20) laser output was used to generate Ag vapor from a surface of a rotating and translating silver rod. The produced Ag vapor was cooled in a channel (40 mm long and 3 mm diameter) to form  $\text{Ag}_n\text{F}_m^+$  cluster cations by He gas with a mixture of 5%  $\text{SF}_6$  expanded from a pulse valve (General Valve, Series 9). The cluster beam was introduced into a second chamber through a conical skimmer. In the second chamber, the injected cluster ions were accelerated by pulsed electric fields in a Wiley-McLaren-type TOF mass spectrometer. In the first field free region of the TOF mass spectrometer, cluster ions with a given mass-to-charge ratio were selected by a pulsed mass gate. The selected ions were photolyzed by another pulsed laser, which was irradiated perpendicularly with the cluster-ion beam direction before the ions entered the reflection region of the reflectron. The produced photofragment and remaining parent ions were then mass analyzed in the reflection region and in the second field

<sup>a</sup> e-mail: misaizu@qpcrkk.chem.tohoku.ac.jp

free region, and they were detected by a dual microchannel plate detector (MCP, Hamamatsu F1552-21S). The second harmonic of a pulsed Nd:YAG-pumped dye laser (Spectra-Physics, GCR-150 and Sirah, GSTR-G-24) was used as a photolysis laser to generate photons with wavelengths of 219–330 nm by using a frequency doubling system (Inrad, Autotracker III). The photodissociation spectrum was obtained by measuring the photofragment ion intensity, which was normalized by laser fluence and by the parent ion intensity, as a function of photon energy.

### 3 Calculation

The ground state geometry of  $\text{Ag}_2\text{F}^+$  was optimized by a theoretical calculation based on density functional theory (DFT) using the B3LYP functional with the Gaussian03 package [15]. The basis set of MWB28 (effective core potential for core electrons  $1s$  to  $3d$ ) [16] was used for the silver atom, and  $6\text{-}31\text{+G}^*$  was used for F. Natural population analysis for the optimized structures was also performed in order to estimate charge distributions in the clusters. We also calculated the electron excitation energies from the ground state with time-dependent density functional theory (TDDFT) method [17].

### 4 Results and discussion

Figure 1a shows a typical TOF mass spectrum of silver fluoride cluster ions. In this mass spectrum, the ion series corresponding to  $\text{Ag}_n\text{F}_{n-1}^+$  were observed most intensely. This type of ions in which the number of the metal atom is larger by one than that of the halogen atom, was also observed typically in mass spectra of alkali halide cluster ions. The alkali-halide clusters are known to be composed of alkali metal cations and halogen anions [18], and thus the total charge of the clusters are in most cases determined by the difference between the number of alkali metal and halogen atoms. Because the silver atom, having a similar electron configuration to alkali atoms with one s-valence electron, exists as an  $\text{Ag}^+$  ion in various complexes, the observed feature implies that silver fluoride cluster ions consist of  $\text{Ag}^+$  and  $\text{F}^-$ . We also detected other type of ions assignable to  $\text{Ag}_n\text{F}_{n-2}^+$  and  $\text{Ag}_n\text{F}_{n-3}^+$ . These ions were also detected as a predominant series in silver bromide cluster ions reported by L'Hermite et al. [7].

Mass spectra of photofragment ions from  $\text{Ag}_n\text{F}_{n-1}^+$  were obtained for  $n = 2\text{--}8$  by taking the difference between mass spectra with photolysis laser-on and those with laser-off. Figures 1b and 1c show examples of such photofragment-ion mass spectra for  $n = 2$  and 6 at a photolysis wavelength of 266 nm. Silver atom has two isotopes,  $^{107}\text{Ag}$  and  $^{109}\text{Ag}$ , in the natural abundance of 51.2:48.2. Thus we selected the most abundant species as a parent ion in the photodissociation of  $\text{Ag}_n\text{F}_{n-1}^+$ . In these mass spectra, predominant photodissociation pathway from the ion of  $n = 2$  was the F-atom loss:

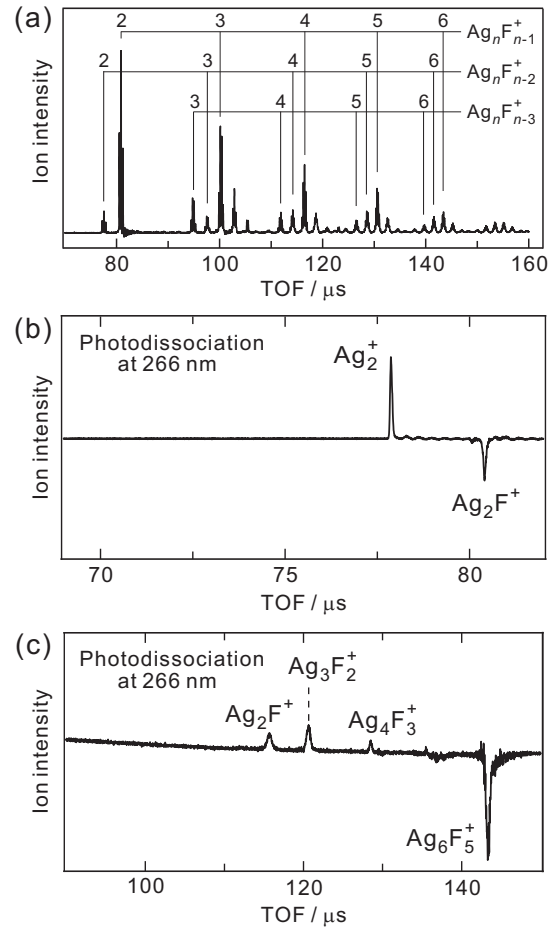
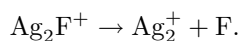
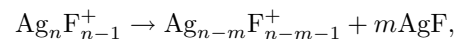


**Fig. 1.** Typical mass spectrum of (a) silver fluoride cluster cations and the photodissociation difference mass spectra from the photolysis laser on-minus-off of (b)  $\text{Ag}_2\text{F}^+$  and (c)  $\text{Ag}_6\text{F}_5^+$  at a dissociation wavelength of 266 nm.

By contrast, dissociation reaction of  $\text{AgF}$ -units,



was observed most prominently from other cluster ions for  $n = 3\text{--}8$ . Both fragmentation reactions, F-atom loss and  $\text{AgF}$  loss, were observed from the ions of  $n = 3$  and 4, although the fraction of F-atom loss was found to be insignificant. As cluster size increases, losses of  $\text{AgF}$  units became predominant, and no fragment ions produced by dissociation of F atoms were observed at  $n = 5\text{--}8$ . Based on these experimental observations, the photodissociation spectrum of  $\text{Ag}_2\text{F}^+$  was obtained by monitoring  $\text{Ag}_2^+$  ion intensity as a function of photolysis energy, as shown in Figure 2. Several sharp bands were observed in the photolysis energy region of 3.8–5.6 eV.

DFT calculations of  $\text{Ag}_2\text{F}^+$  were performed in order to get information on the fragmentation processes and excited states observed in the photodissociation spectrum. We first obtained a ground state structure of  $\text{Ag}_2\text{F}^+$  as shown in Figure 3. The ground state was found to be a singlet  $^1\Sigma_g^+$  state with a linear Ag-F-Ag geometry ( $D_{\infty h}$  symmetry) in which an Ag-F distance is 2.12 Å [Fig. 3a].

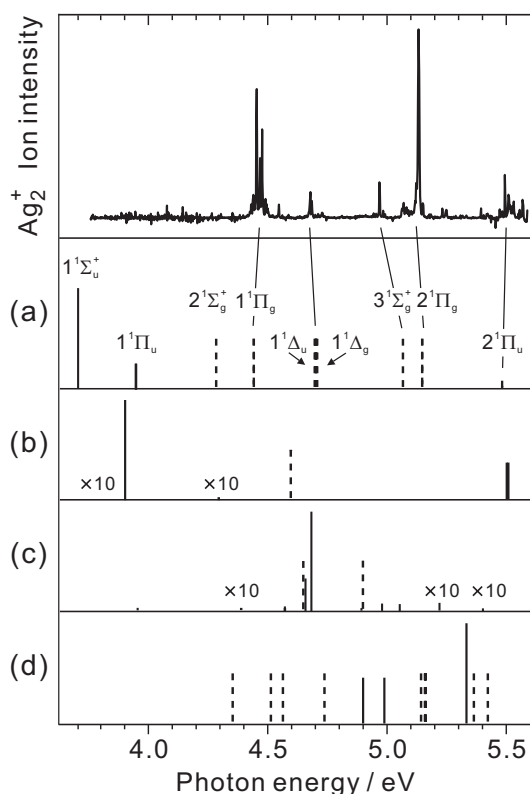


**Fig. 2.** Photodissociation spectrum of  $\text{Ag}_2\text{F}^+$  (top) and the results of TDDFT calculations for (a) linear  $[\text{Ag-F-Ag}]^+$  in the singlet state and for triplet states of (b) linear  $[\text{Ag-Ag-F}]^+$ , (c) bent  $[\text{Ag-F-Ag}]^+$ , and (d) linear  $[\text{Ag-F-Ag}]^+$ . For (a)–(d), the vertical axis corresponds to the oscillator strength, and broken lines show the bands of which oscillator strengths are vanishing because of optically forbidden transitions.

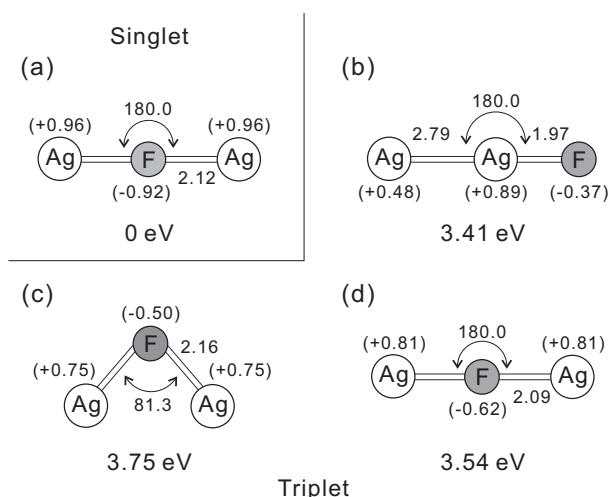


**Fig. 3.** Optimized structures, natural charges (in parentheses) and relative energies of (a) linear  $[\text{Ag-F-Ag}]^+$  in the singlet state, and triplet states of (b) linear  $[\text{Ag-Ag-F}]^+$ , (c) bent  $[\text{Ag-F-Ag}]^+$ , and (d) linear  $[\text{Ag-F-Ag}]^+$  calculated by B3LYP/MWB28 for Ag and 6-31+G\* for F. Bond lengths and angles are shown in angstrom and degrees, respectively.

On the other hand, Rabilloud et al. reported a calculation result that  $\text{Ag}_2\text{Br}^+$  has a bent Ag-Br-Ag structure ( $C_{2v}$ ) [11]. Natural population analysis shows that the former ions are composed of silver cations and a fluoride anion; natural charges of Ag and F atoms in  $\text{Ag}_2\text{F}^+$  are estimated to be +0.96 and –0.92 respectively. This result is in good agreement with the experimental results in the mass spectra that the  $\text{Ag}_n\text{F}_{n-1}^+$  was observed as a predominant ion series. The difference in geometry between  $\text{Ag}_2\text{F}^+$  and  $\text{Ag}_2\text{Br}^+$  can be explained from the balance of the interatomic interactions between silver and halogen ions, an electrostatic (Coulomb) interaction and an orbital interaction. In the case of  $\text{Ag}_2\text{F}^+$ , energy gap between Ag 5s and F 2p is too large to interact with each other. Thus,  $\text{Ag}_2\text{F}^+$  has a linear structure as a result of Coulomb interaction. On the other hand, Br 4p orbitals, lying at higher energy compared with F 2p, can interact with Ag 5s and 4d orbitals. As a result of these orbital interactions,  $\text{Ag}_2\text{Br}^+$  has a bent structure [11]. There are no isomers except for linear Ag-F-Ag in the singlet ground state of  $\text{Ag}_2\text{F}^+$ . On the other hand, three different isomers, a Ag-Ag-F linear isomer, a Ag-F-Ag linear isomer, and a Ag-F-Ag bent isomer, were found for the triplet state as shown in Figures 3b–3d. However, the coexistence of these triplet isomers is improbable, because the energies of these triplet isomers are considerably (at least 3.4 eV) higher than the  $^1\Sigma_g^+$  ground state.

Excitation energies of  $\text{Ag}_2\text{F}^+$  from the singlet and triplet isomer states were next calculated by TDDFT method with the same basis sets. We found several electronically excited states in the examined UV region for all isomers. Among these, excitation energies from the singlet state were found to be in the best agreement with those of the observed bands in the dissociation spectrum as shown in Figure 2. Therefore we safely excluded the possibility of the coexistence of the triplet isomers, in addition to the energetics consideration noted above. The observed bands are all assignable to the electron excitations from the molecular orbital composed of  $\text{Ag}^+$  4d and  $\text{F}^-$  2p to  $\text{Ag}^+$  5s. We showed the state labeling of the linear geometry in the figure. From the  $^1\Sigma_g^+$  ground state, electric dipole transitions are only allowed to the states of  $^1\Sigma_u^+$  and  $^1\Pi_u$ . The lowest two allowed transition bands to the  $^1\Sigma_u^+$  and  $^1\Pi_u$  states were not observed due to the insufficient energy for dissociation; the total energy difference between the parent  $\text{Ag}_2\text{F}^+$  ion and the products,  $\text{Ag}_2^+$  and F, was calculated to be 3.90 eV. Probably the transition to the third  $^2\Sigma_g^+$  excited state was not observed for the same reason. In contrast, transitions to all excited states higher than 4.45 eV were observed in the photodissociation spectrum, all of which are forbidden except for the transition to the  $^2\Pi_u$  state at 5.5 eV. This is probably because the selection rule is easily broken by vibrational excitation of the parent ion. The energy of the bending vibration in the  $\text{Ag}_2\text{F}^+$  ground state was calculated to be  $80\text{ cm}^{-1}$ , and thus the excitation of such a low frequency mode may be probable for the present laser-vaporization source. Most of the forbidden transitions in linear geometry turn out to be allowed from the bent  $A_1$  ground state. In particular, the

$^1\Pi_g$  excited states, which are very prominent in the spectrum, were found to gain transition intensities by coupling with the allowed  $^1\Sigma_u^+$  state under the bending vibrational excitation.

In the fragmentation process of the centered F atom from the linear  $\text{Ag}_2\text{F}^+$  ion, it is necessary to change the geometry by further excitation of a bending vibration. We first expected that this bending vibration is excited further in excited electronic states to promote the dissociation, and so we obtained potential energy curves of the ground and several excited states by plotting energies along the Ag-F-Ag bond angle  $\theta$ . In this calculation, the Ag-F bond length was optimized at every bond angle. As a result, contrary to our expectation, all of the excited-state potential-energy curves have minima at  $\theta = 180$  degrees, which are similar to that of the ground state. This result indicates that for all excited states examined, the parent  $\text{Ag}_2\text{F}^+$  ion has linear equilibrium geometries similar to the ground state, and that the  $\text{Ag}_2^+$  and F fragments are not produced directly from the excited states. Therefore, the F atom is expected to be fragmented as a result of internal conversion from the excited electronic states to higher vibrational levels of the ground state and the following conformational changes. This fragmentation pathway via nonradiative internal conversion is reasonable as a relaxation process from the excited state with a small oscillator strength, because the radiative relaxation is suppressed from this state. This indirect, predissociative fragmentation reaction mechanism is also consistent with the sharp band features observed in the photodissociation spectrum. There is also a possibility that the disagreement between the observed band intensity and the calculated oscillator strength is due to the state-dependence of the efficiency of internal conversion and fragmentation. In the dissociation from the high vibrational states of the ground state of  $\text{Ag}_2\text{F}^+$ , the ground electronic potential surface is further necessary to be crossed with a kind of charge-transfer state. At the smaller bending angle corresponding to the smaller Ag<sub>2</sub>-F distance, each atomic ion keeps its charge. As a result, the ground potential curve correlates with a dissociated pair of  $\text{Ag}_2^{2+} + \text{F}^-$  which lies more than 8 eV above the ground state. However, at some increased Ag<sub>2</sub>-F distance this potential should be crossed with the state having a charge-transfer character correlating with the  $\text{Ag}_2^+ + \text{F}$  reaction products, which lies at 3.9 eV above the original ground state.

There still remains a question why the fragmentation reaction of  $\text{Ag}_2\text{F}^+ \rightarrow \text{Ag}_2^+ + \text{F}$  was observed as the only dissociation pathway. We investigated energies necessary for other possible dissociation reactions and constructed an energy diagram. The energetically lowest dissociation pathway is the production of  $\text{Ag}^+ + \text{AgF}$ , in which the dissociation energy of 2.33 eV is much smaller than that of producing  $\text{Ag}_2^+$ . At all cluster sizes larger than  $n = 2$ , this

type of fragmentation losing a AgF-unit was observed as predominant dissociation channel. There is also another question of how the bending vibration is excited to fragment the centered F atom. Probably these two questions are related to each other. In order to elucidate these issues, it is necessary to unveil the full potential energy surfaces of the ground state and the relevant excited states.

This work has been supported in part by a Grant-in-Aid for Scientific Research from the Japanese Ministry of Education, Culture, Sports, Science and Technology. The computations were partly performed using Research Center for Computational Science, Okazaki, Japan. We also thank S. Maeda for his helpful suggestions of potential energy curves and computational techniques.

## References

1. B. Zemva, K. Lutar, A. Jesih, W.J. Casteel, A.P. Wilkinson, D.E. Cox, R.B. Von Dreele, H. Borrmann, N. Bartlett, *J. Am. Chem. Soc.* **113**, 4192 (1991)
2. K. Edamatsu, G. Oohata, R. Shimizu, T. Itoh, *Nature* **431**, 167 (2004)
3. P.D. Mitev, M. Saito, Y. Waseda, *Mater. Trans.* **42**, 829 (2001)
4. A.D. Cicco, M. Taglienti, M. Minicucci, A. Filipponi, *Phys. Rev. B* **62**, 12001 (2000)
5. D.L. Hildenbrand, K.H. Lau, *J. Phys. Chem. A* **109**, 11328 (2005)
6. H. Zhang, Z.A. Schelly, D.S. Marynick, *J. Phys. Chem. A* **104**, 6287 (2000)
7. J.M. L'Hermite, F. Rabilloud, L. Marcou, P. Labastie, *Eur. Phys. J. D* **14**, 323 (2001)
8. J.M. L'Hermite, F. Rabilloud, P. Labastie, F. Spiegelman, *Eur. Phys. J. D* **16**, 77 (2001)
9. G.J. Stueber, M. Foltin, E.R. Bernstein, *J. Chem. Phys.* **109**, 9831 (1998)
10. C.J. Evans, M.C.L. Gerry, *J. Chem. Phys.* **112**, 1321 (2000)
11. F. Rabilloud, F. Spiegelman, J.M. L'Hermite, P. Labastie, *J. Chem. Phys.* **114**, 289 (2001)
12. H.-C.M. Rösing, A. Schulz, M. Hargittai, *J. Am. Chem. Soc.* **127**, 8133 (2005)
13. A. Ramírez-Solís, *J. Chem. Phys.* **120**, 2319 (2004)
14. A. Ramírez-Solís, J.P. Daudey, *J. Chem. Phys.* **113**, 8580 (2000)
15. M.J. Frisch et al., *Gaussian 03*, revision B.04 (Gaussian, Inc., Pittsburgh PA, 2003)
16. D. Andrae, U. Häußermann, M. Dolg, H. Stoll, H. Preuß, *Theor. Chim. Acta* **77**, 123 (1990)
17. M.E. Casida, in *Recent Advances in Density Functional Methods Part I*, edited by D.P. Chong (World Scientific, Singapore, 1995)
18. R.L. Whetten, *Acc. Chem. Res.* **26**, 49 (1993)